Development of an Operational State observer for Power Assist Wheelchair

Sehoon Oh [a] and Yoichi Hori [a]

[a] Department of Electrical Engineering, University of Tokyo, 4-6-1 Komaba Meguro, Tokyo, 192-0914, Japan

sehoon@horilab.iis.u-tokyo.ac.jp, hori@iis.u-tokyo.ac.jp

***Abstract* - Two kinds of operational state observer for a wheelchair system is proposed in this paper. The observer can estimate three main physical values: (1) the speed of the wheelchair, (2) the leaning angle of the wheelchair body from the ground and (3) external disturbances. The observer can sensorfuse the information from three sensors - accelerometer, encoder, gyroscope - using the kalman filter theory. The observer is extended to three dimensions incorporating a 3-axis accelerometer and allows the user to estimate more precise information on conditions of hills for the lateral direction. To this end, dynamics model of a wheelchair and output equation of each sensor are derived and simplified. Then, the Kalman filter theory enables us to integrate sensors. Experimental results verify the stability and effectiveness of the proposed operational state observer.**

***Keywords* - wheelchair, operational state observer, Kalman filter, friendly motion control.**

I. Introduction

Nowadays advanced power assist devices are drawing people's attention as emerging control application [1]. A power assist wheelchair is a good example of the assist devices [2]. In conventional power assist wheelchairs, motors just multiply original human force by up to several times [3]. But, a power assist wheelchair needs to change its assistance according to the environment where it locates. For example, when a wheelchair goes on a hill, assisting motors should decrease its assist ratio in order to prevent tipping over of a wheelchair.

This means that power assist system should distinguish the road condition and identify the states of the wheelchair. This is the reason why the operational state observer becomes necessary.

As basic operational states of a wheelchair, three kinds of physical value are used: the linear velocity, pitch angle of a wheelchair and external force applied to a wheelchair. We call these one dimensional states as linear operational states. These linear states can also provide information on the angle of a slope where a wheelchair is located on in the direction to which the wheelchair is headed. Additionally, the lateral angle of the slope is another important operational state. All these states can be estimated correctly using the operational state observer proposed in this paper.

In Section II and III, an observer for linear operational states is developed and verified by experiments.

Fig.1. Power assist wheelchair as an experimental setup (YAMAHA JW II)

In Section III and IV, the linear operational state observer is extended to three dimensions and enables us to obtain more precise two dimensional information on a slope where a wheelchair is locate.

II. Development of Observer for Linear Operational States of Wheelchair

A. Description of Operational States of Power Assist Wheelchair

Driving speed (v_f in Fig. 2 (a)) and inclination angle (θ_p in Fig. 2 (a)) are important information in controlling a wheelchair. The driving speed means the speed of the whole wheelchair and it is in a parallel direction with the ground, which is illustrated in Fig. 2 (a). Inclination angle is the leaning angle of the wheelchair frame from the horizon. If the wheelchair is on a level ground this angle becomes zero, but if the wheelchair is on a slope or the frame of the wheelchair is inclined against the ground, this angle has non-zero value.

The location of this inclination angle on a phase plane can indicate the stability of the wheelchair in the pitch direction. If a controller can use the value, it will make the rider feel comfortable even when the wheelchair is on a hill.

Encoders usually measure the driving speed. It should be noted that the wheelchair repeats low speed driving and stops. Speed measurements at low or zero speed are liable to be noisy and incorrect when we use encoders for measurements. An observer proposed in this paper can estimate these two values correctly and make them available for a feedback control.

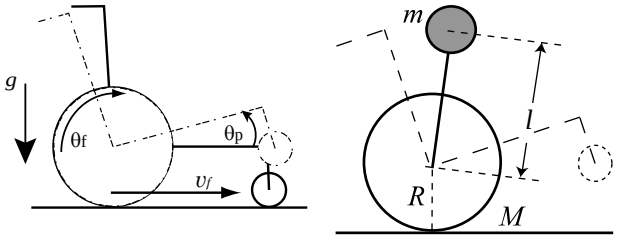

(a) states of wheelchair (b) inverted pendulum model

Fig.2 Physical Values Needed for Control

A. Observer Design Using Kalman Filter Theory

In order to design the required observer, states in equation (1) are adopted. ω_p, ω_f are the velocities of θ_p, θ_f. θ_p is the inclination angle explained previously. θ_f is the rotated angle of a wheel. Driving speed v_f can be calculated by $v_f = R\omega_f$ ignoring slips on wheels (R is the radius of the wheel). Lastly d_p, d_f are the disturbances exerted on θ_p, θ_f respectively.

$$x = \begin{pmatrix} \omega_p & \omega_f & \theta_p & \theta_f & d_p & d_f \end{pmatrix}^T \quad (1)$$

Motion equations of these states are shown in equation (2).

$$J_f\ddot{\theta}_f = -B_f\dot{\theta}_f + \tau_f + d_f, J_p\ddot{\theta}_p = -B_p\dot{\theta}_p + d_p, v_f = R\theta_f \quad (2)$$

J_f, J_p, B_f, B_p are inertias and dampings in each state. τ_f is the torque to propel the wheel, and it is exerted by human or motor. This equation uses disturbance terms to simplify the equation. The input torque to θ_p is set as 0, and θ_p is excited only by disturbance d_p. This enables us to ignore the restriction by the connection between θ_p and θ_f .extremely simplified forms using the disturbances d_f, d_p.

Equation (3) and (4) show detailed form of these equations. These equations are derived based on the inverted pendulum model

$$\tau_f + d_f = \{(M+m)r + J_M\}\ddot{\theta}_f - mlr\ddot{\theta}_p\cos\theta_p + mlr\dot{\theta}_p^2\sin\theta_p + B_M\dot{\theta}_f \quad (3)$$

$$d_p = \left(J_m + ml^2\right)\ddot{\theta}_p - mlr\ddot{\theta}_f\cos\theta_p - mgl\sin\theta_p \quad (4)$$

M is the weights of wheels of wheelchair and *m* is the weight of the body including a rider. *l* is the distance of the center of gravity of the body from the axis of wheels. *g* is the gravity acceleration (See Fig.2 (b)). We can notice that the former motion equations are in extremely simplified forms using the disturbances d_f, d_p compared with the latter equations.

[4] shows that these two types of equations do not make any difference in estimation. In this paper, simplified equation (2) is employed.

B. Sensors and Output Equations

Three sensors (encoder, gyroscope, and accelerometer) are used for measurements. Output equations are shown in Table I.

TABLE I

OUTPUT EQUATION OF EACH SENSOR

Encoder	$y_{\text{enc}} = \theta_f$
Gyroscope	$y_{\text{gyro}} = \omega_p$
Accelerometer	$y_{\text{acc}_x} = R\dot{\omega}_f\cos\theta_p + g\sin\theta_p$
	$y_{\text{acc}_y} = g\cos\theta_p - R\dot{\omega}_f\sin\theta_p$

The measurements a_x and a_y in the accelerometer are described in Fig. 3. a_x should be linearized to be utilized in the kalman filter. This results in the output equation for the observer shown in Equation (5).

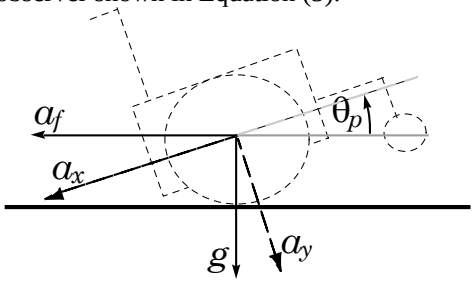

Fig. 3. Accelerations measured by accelerometer

$$y = \begin{pmatrix} \omega_p & \theta_f & a_x \end{pmatrix}^T = \begin{pmatrix} 1 & 0 & 0 & 0 & 0 & 0 \\ 0 & 0 & 0 & 1 & 0 & 0 \\ 0 & -\frac{BR}{J} & g & 0 & 0 & \frac{R}{J} \end{pmatrix} x + \begin{pmatrix} 0 \\ 0 \\ \frac{R}{J} \end{pmatrix} u \quad (5)$$

The observer has three outputs, which makes the decision of observer gain not so simple. We adopted the kalman filter method for the calculation of the observer gain.

III. VERIFICATION OF PROPOSED LINEAR OPERATIONAL OBSERVER BY EXPERIMENT

Due to the limitation of sensors, the measurements of ω_f and θ_p can be incorrect. In order to get ω_f information, we should differentiate the encoder output discretely. If the resolution of the encoder is too low or the angular velocity of the wheel is too low, the discretely differentiated velocity will be very noisy and incorrect. To overcome this, a low pass filter is utilized, but it will make the estimation slow.

And for the measurement of θ_p, the value of a gyroscope is integrated. If there is some noise in the output of the gyroscope, the drift phenomenon will occur.

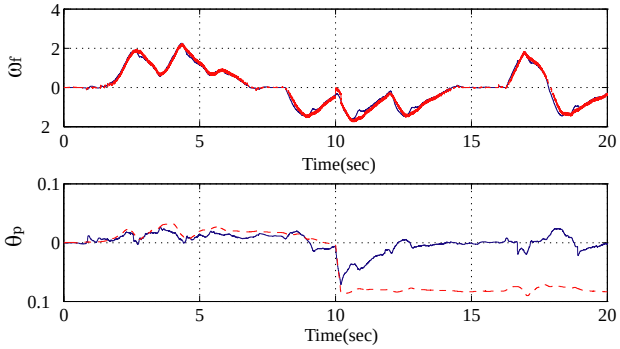

(a) On level ground

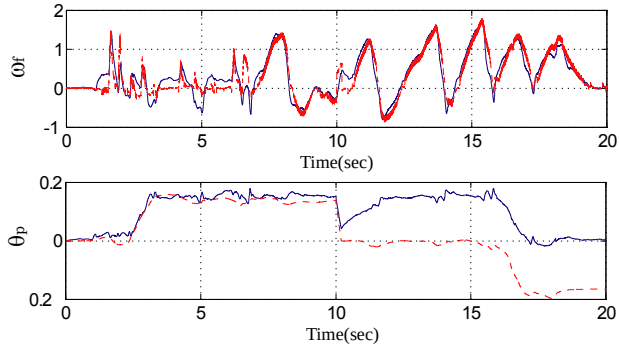

(b) On a slope

Fig.4. Estimated States: $\hat{\omega}_f$ and $\hat{\theta}_p$

Proposed observer can overcome these two problems. Experimental results shown in Fig. 4 explain this point. Each figure shows ω_f and θ_p respectively. In (a), the wheelchair runs straightly on a level ground, while (c) shows the result of experiment where at 10 second, a wheelchair goes on a slope. The dotted line in the upper figure of each experiment which shows ω_f, is the low pass filtered differential of the encoder output. This value is very noisy and delayed, while the estimation of the proposed observer (solid line) is fast and not noisy. To investigate the robustness of proposed observer, we added a noise to the gyroscope output at 10 sec. Let's see the below figure of each experiment. This shows the estimated θ_p. Compared to the integration of the gyroscope output (dotted line in the below figure of each experiment), the proposed observer estimation (solid line) shows robust observation results. From this experimental result, we can conclude that using the proposed observer, the drift phenomenon can be avoided and better velocity information will be obtained.

We can identify the states of the wheelchair using this estimated θ_p, and apply this information to the control. But the inclination angle is not sufficient to tell whether it is on a slope or during a wheelie. d_f will tell this information. Fig. 5 is the estimated d_f s. The left figure is $\hat{d}_f$ on a slope, and the right is $\hat{d}_f$ during a wheelie.

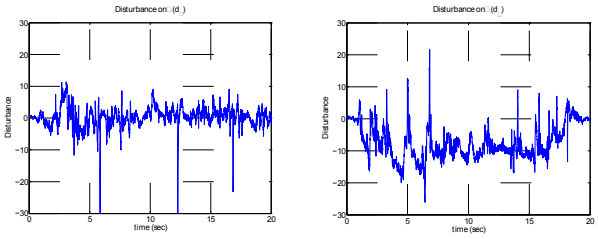

(a) states of wheelchair (b) inverted pedulum model

Fig.5. Estimated States: $\hat{\omega}_f$ and $\hat{\theta}_p$

If the wheelchair is on a slope, the gravity act as a disturbance to driving, but if the wheelchair is during a wheelie, it is not. Using this $\hat{d}_f$, more classified identification of the wheelchair states is available.

IV. Description of Three-dimensional Operational State

A. Extension of Operational State Observer Equations

Since the linear operational state observer employs a two-dimensional accelerometer, any information on the lateral direction is not measurable. The gravity acting in the lateral direction, illustrated in Fig. 6 will not be estimated in this observer. However, as this lateral gravity interferes with the heading direction of a wheelchair making the wheelchair turn regardless of the user's will. In order to improve the manipulability, information of this lateral gravity comes necessary.

This necessary information can be represented as the values described in Fig. 6: the pitch angle of a wheelchair (φ) with regarding to its heading direction, the heading angle (α) with regard to the horizon and the slope angle (ξ) of a hill.

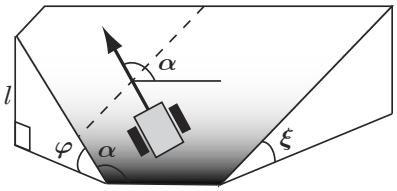

Fig.6. Angles Necessary for Safe Operation on a Slope

In order to design a Kalman that estimates these angles, the relationship between the measured values and operational states, especially the angles to be estimated should be analyzed at first. This analysis will be done later.

B. Derivation of Output Equations Produced by Three Sensors Equations

Three kinds of sensors are utilized in this system: one 3-axis accelerometer, two encoders on both wheels and one gyroscope that measures the pitch angle around the axis of wheels. These sensors provide φ, α and ξ in Fig. 6 and the moving velocity v_f in Fig 2 (a).

Fig. 6 shows the relationship between the pitch angle φ and the yaw or heading angle α of a wheelchair on a slope of ξ. This relationship will be described as Equation (6).

$$\sin\varphi = \sin\alpha \sin\xi \tag{6}$$

This equation reveals the output equation of the gyroscope which measures the angular velocity of φ. The equation is given as Equation (8).

$$\varphi = \sin^{-1}(\sin\alpha \sin\xi) \cong \sin\alpha \sin\xi \tag{7}$$

$$\dot{\varphi} \cong \dot{\alpha}\cos\alpha \sin\xi + \dot{\xi}\sin\alpha\cos\xi \tag{8}$$

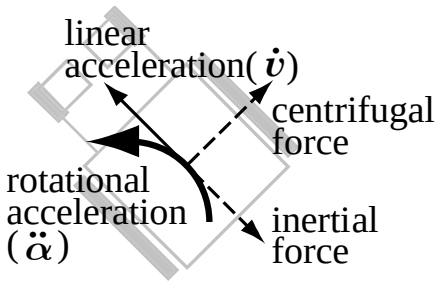

Fig.7. Decomposition of the force measured by an accelerometer

Accelerometer measures the linear acceleration of the wheelchair including the gravity vector. In addition to the heading acceleration in the linear direction, yaw acceleration is also measured by 3-axis acceleration. Equations (9) to (11) describe the output equations of a 3-axis accelerometer.

$$a_x = g\sin\xi\sin\alpha + \dot{v} + f_{\text{rotation}_x} \tag{9}$$

$$a_y = g\sin\xi\cos\alpha + v\dot{\alpha} + f_{\text{rotation}_y} \tag{10}$$

$$a_z = g\cos\xi, \tag{11}$$

where v illustrates the velocity of a wheelchair in its heading angle. The directions of x, y, z axes are illustrated in Fig. 8.

The first term of each equation shows the gravity vector of which direction is determined by the condition α, ξ of a hill the wheelchair is located. The second terms represent the inertial force in Equation (9) and the centrifugal force in Equation (10). These are the forces manifested on the center of mass.

Meanwhile, $f_{\text{rotation}_{x,y}}$ are the forces caused by the fact that the accelerometer is not located in the center of mass of the wheelchair. Rotational motion around the center of mass produces additional acceleration measurements in the accelerometer. Fig. 8 (a) shows the location of the accelerometer in a wheelchair. Since it is Δ_x, Δ_y off the center, additional inertial and centrifugal forces are applied to the accelerometer described in Equation (12) and (13).

$$f_{\text{rotation}_x} = \ddot{\alpha}\Delta_x + m\dot{\alpha}^2\Delta_y \tag{12}$$

$$f_{\text{rotation}_y} = -\ddot{\alpha}\Delta_y + m\dot{\alpha}^2\Delta_x \tag{13}$$

First terms are the output of the inertial force and second terms are the output of the centrifugal force. Notice that Δ_y would be 0 if v is calculated as the linear velocity at the location of the accelerometer.

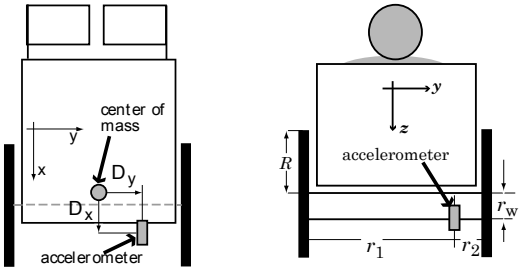

(a) Top view (b) Rear view

Fig.8. Location of an Accelerometer in a Wheelchair

If the slip between the wheels and the ground is ignored, the rotated angles of two wheels which are represented as θ_l, θ_r can be associated with the measured acceleration. v at the location of the accelerometer is identified with Equation (14) using θ_l, θ_r.

$$v = \frac{r_2}{r_1 + r_2} R\dot{\theta}_r + \frac{r_1}{r_1 + r_2} R\dot{\theta}_l, \tag{14}$$

where r_1, r_2, R means the lengths and distances illustrated in Fig. 8. Also the heading angle α in Equation (10) can be derived from θ_l and θ_r as Equation (15) assuming no slip.

$$\alpha = \frac{R}{r_1 + r_2}(\theta_r - \theta_l) \tag{15}$$

Finally we obtain 6 output equations of all sensors, which contain the values of φ, α, ξ we want to estimate. The equations are re-described in Table II.

TABLE II

OUTPUT EQUATION OF EACH SENSOR

Gyroscope	$\dot{\varphi} = \dot{\alpha}\cos\alpha\sin\xi + \dot{\xi}\sin\alpha\cos\xi$
Accelerometer	$a_x = g\sin\xi\sin\alpha + \dot{v} + m\dot{\alpha}^2\Delta_y$ $a_y = g\sin\xi\cos\alpha + v\dot{\alpha} - \ddot{\alpha}\Delta_y$ $a_z = g\cos\xi$
Encoder	$v = \frac{r_2}{r_1+r_2}R\dot{\theta}_r + \frac{r_1}{r_1+r_2}R\dot{\theta}_l$ $\alpha = \frac{R}{r_1+r_2}(\theta_r - \theta_l)$

B. Derivation of Three-dimensional Dynamics [5]-[7]

A precise modeling of dynamics that is necessary to describe how external force or the gravity affects on the motion of a wheelchair in the lateral direction is derived in this section. Since the lateral disturbance affects on the lateral motion of the wheelchair through the tires, the model should include the cornering force of the tires. This point is quite similar with the analysis on the dynamics of four-wheel vehicle. For this similarity, the modeling of vehicle dynamics is adopted to explain the lateral motion of a wheelchair.

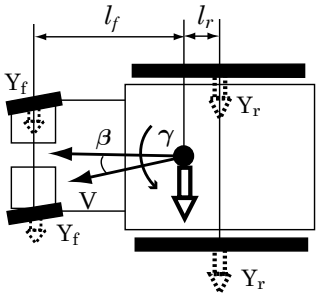

Fig.9. Lateral Motion of a Wheelchair

Fig. 9 shows the relationship between the direction of moving velocity and heading direction. The difference is called as β or the slip angle in the vehicle engineering. When the gravity acts on the wheelchair in the lateral direction, that lateral force brings about the slip angle causing tire to produce cornering force. Finally the gravity results in the change of the heading angle. This relationship between the dynamics of β and the yaw rate γ is described in Equation (16) and (17).

$$mV\left(\frac{d\beta}{dt}+\gamma\right)=Y_f(\beta_f,\gamma)+Y_r(\beta_r,\gamma)+g_{\text{lat}} \tag{16}$$

$$I\frac{d\gamma}{dt}=l_fY_f(\beta_f,\gamma)-l_rY_r(\beta_r,\gamma), \tag{17}$$

where Y_f, Y_r mean the cornering force acting on the front wheels and the real wheels (Fig. 9).

Since the front wheels of a wheelchair consist of casters and are not fixed so that the heading angle of the front wheels can be identified with the direction of the wheelchair's moving velocity, V in Fig. 7. This means β s in the front wheels is quite small and there will be little cornering force in the front wheels. Based on this assumption, the cornering forces Y_f, Y_r are given as the following.

$$Y_f=-K_f\beta_f \quad = \quad 0 \tag{13}$$

$$Y_r=-K_r\beta_r \quad = \quad -K_r\left(\beta-l_r\frac{\gamma}{V}\right) \tag{14}$$

Based on this consideration, the transfer function from the gravity to the rotated angle $\alpha=\int\gamma dt$ which we want to estimate, is given as a second order system. It, however, can be approximated to a first order time delay system in Equation (15), considering that the gravity does not changes so drastically that its frequency band is not high.

$$\frac{\gamma}{g_{\text{lat}}}=\frac{\dot\alpha}{g_{\text{lat}}}=\frac{K}{s^2+2\zeta\omega_n s+\omega_n^2}\rightarrow\frac{K}{s+\omega_o} \tag{19}$$

$$\ddot x_l=-\frac{D}{M}\dot x_l+\frac{1}{M}(u_f-Mg\sin\alpha\sin\xi) \tag{20}$$

$$\ddot\alpha=-\frac{B}{I}\dot\alpha+\frac{1}{I}(u_\tau-Mgl_r\cos\alpha\sin\xi) \tag{21}$$

Equation (22) and (24) show the whole system dynamics equation and output equation.

$$x=\begin{pmatrix}x_l & \alpha & \dot x_l & \dot\alpha & \xi & \dot\xi\end{pmatrix}^T=\begin{pmatrix}x_1 & x_2 & x_3 & x_4 & x_5 & x_6\end{pmatrix}^T \tag{22}$$

$$x=\begin{pmatrix}x_3\\ x_4\\ -\frac{D}{M}x_3-g\sin x_2\sin x_5\\ -\frac{B}{I}x_4-\frac{M}{I}g\cos x_2\sin x_5\\ x_6\\ 0\end{pmatrix}+\begin{pmatrix}0\\0\\\frac{1}{M}u_f\\\frac{1}{I}u_\tau\\0\\0\end{pmatrix}=f(x)+g(u) \tag{23}$$

$$y=\begin{pmatrix}x_1\\x_2\\x_4\cos x_2\sin x_5+x_6\sin x_2\cos x_5\\\dot x_3+g\sin x_2\sin x_5+m_{acc}d_{accx}x_4^2\\Mx_3x_4+g\cos x_2\sin x_5+m_{acc}d_{accy}x_4^2\\g\cos x_5\end{pmatrix}=\begin{pmatrix}x_1\\x_2\\x_4\cos x_2\sin x_5+x_6\sin x_2\cos x_5\\-\frac{D}{M}x_3+m_{acc}d_{accx}x_4^2+\frac{1}{M}u_f\\Mx_3x_4+g\cos x_2\sin x_5+m_{acc}d_{accy}x_4^2\\g\cos x_5\end{pmatrix}=h(x,u) \tag{24}$$

Kalman filter design is adopted for the design of the state observer due to the characteristics of the motion and output equations: at first, it has multi-output so that it is not easy to decide the observer gain using pole assignment. Secondly, the dynamics has nonlinear characteristic. Extended Kalman filter (EKF) design can deal with these characteristics.

V. Verification of Proposed Extended Operational Observer by Simulation Results

Main purposes of simulations conducted in this section are two: one is the verification of observer design, which means it will be checked whether the extended operation states observer can correctly estimate the states in spite of the linearization approximation done in EKF design. The other is the verification of how effect it is to introduce ξ and $\dot\xi$ as states.

Two cases are simulated: 1) a wheelchair goes up a hill perpendicular to the horizon and 2) a wheelchair attempts to change its heading angle on a hill.

At first, when a wheelchair climbs a hill perpendicular to the horizon, the gravity affects only the moving velocity and the state α will keep its value as $\frac{\pi}{2}$.

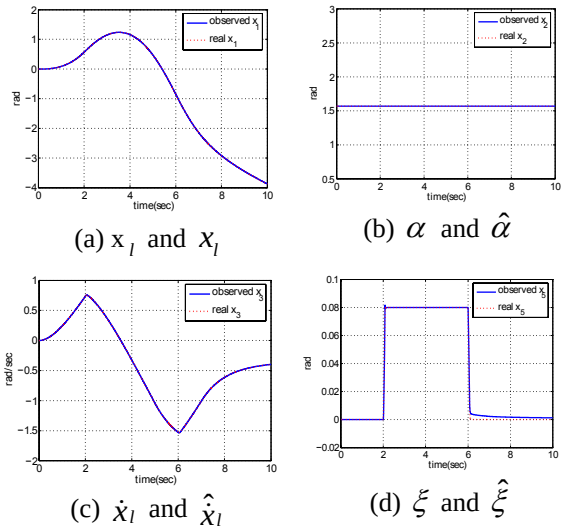

(a) x_l and x_l (b) α and $\hat{\alpha}$

(c) $\dot{x}_l$ and $\hat{\dot{x}}_l$ (d) ξ and $\hat{\xi}$

Fig.11. Simulation 1) Perpendicular Climbing

Fig. 11 shows the result of this perpendicular climbing simulation. Changes in ξ means a wheelchair goes up a hill of 0.08 rad from 2 to 6 second. Since torque to propel a wheelchair in the longitudinal direction is applied to a wheelchair, it starts to move and the state x_l increases for the moment. However, after the wheelchair goes up a hill x_l and $\dot{x}_l$ start to decrease. This is simulated in the result, and we can check that the proposed observer correctly estimates the states.

Fig. 12 is the simulation results of a wheelchair on which a user attempts to change the heading angle at 1.5 and 6.5 seconds. Fig. 12 (f) shows the yaw moment applied by a user.

Around 1.5 second, α starts to increase from $\frac{\pi}{2}$ by the yaw moment. After 2 second, the gravity starts to affect α since it is not perpendicular to the horizon. α increases due to the gravity from 2 to 6 second. After 6 second, the wheelchair is on level ground again and α is only driven by the applied yaw moment.

In this case, the simulation results show that the proposed observer also estimate the states correctly.

5. Conclusion

In this paper, two types of operation states observer for a power assist wheelchair are proposed. First, the linear operational states observer can estimate the linear velocity and the pitch angle of a wheelchair as well as external force. The extended operational state observer can observe heading angle of a wheelchair and the slope angle on which the wheelchair is as well as wheelchair's moving velocity.

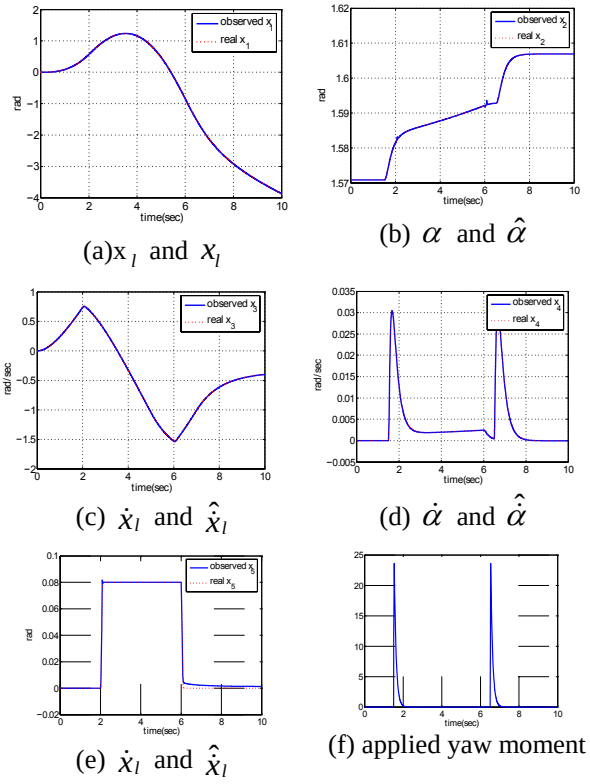

(a)x_l and x_l (b) α and $\hat{\alpha}$

(c) $\dot{x}_l$ and $\hat{\dot{x}}_l$ (d) $\dot{\alpha}$ and $\hat{\dot{\alpha}}$

(e) $\dot{x}_l$ and $\hat{\dot{x}}_l$ (f) applied yaw moment

Fig.12. Simulation 2) Attempts to Change α

For the linear operational states observer, the effectiveness and robustness are evaluated by experimental data. For the extended operational states observer, the effectiveness and the idea of robustness should be implemented to a wheelchair and experimented. This is our future works. The information observed by the proposed observer can realize advanced control of power assist wheelchair[8].

References

[1] R.A. Cooper, "Intelligent Control of Power Wheelchairs" *Engineering in Medicine and Biology Magazine, IEEE*, Vol.14, No. 4, pp.423 - 431, July/Aug,1995

[2] S. Oh and Y. Hori, "Development of Noise Robust State Observer for Power Assisting Wheelchair and its Applications", *IPEC-Niigata*, 2005, pp.1971-1975.

[3] R.A. Cooper, et al., "Evaluation of a Pushrim-Activated, Power-Assisted Wheelchair". *Archives of Physical Medicine and Rehabilitation*, Vol.82, No.5, pp.702-708, May, 2001.

[4] T. Söderström, *Discrete-time Stochastic Systems*, 2002.

[5] C. Guy, B. Georges, and D.N. Brigitte, "Structural Properties and Classification of Kinematic and Dynamic Models of Wheeled Mobile Robots", *IEEE Trans. on Robotics and Automation*, Vol.12, No.1, pp. 47-62, 1996.

[6] C. Luca, D.L. Alessandro, I. Stefano, "Trajectory Tracking Control of a Four-Wheel Differentially Driven Mobile Robot", *Proceedings of the IEEE ICRA*, 1999, Vol.5, pp. 2632-2638.

[7] D. Ding, R.A. Cooper, S. Guo, and T.A. Corfman, "Analysis of Driving Backward in an Electric-Powered Wheelchair", *IEEE Trans. on Control Systems Technology*, Vol.12, No.6, pp. 934-943, 2004.

[8] S. Oh, N. Hata, Y. Hori, “Integrated Motion Control of a Wheelchair in the Longitudinal, Lateral and Pitch Directions” *Proceedings of 9th IEEE AMC*, 2006, pp.2214- 2219